EPR of Ho^{2+} in $SrCl_2$ under uniaxial stress: A parametrization of the orbit-lattice coupling

J. C. Vial and R. Buisson

Laboratoire de Spectrométrie Physique, Université Scientifique et Médicale, B.P. 53, 38041 Grenoble-Cedex, France*

(Received 5 August 1974)

The uniaxial induced shifts of the EPR lines of the ground doublet and of the first-excited doublet of Ho^{2+} in $SrCl_2$ have been measured for various applied stress directions. Although the strong hyperfine structure of Ho^{2+} complicates considerably the calculation, it was possible to show that the results are consistent within the description by a dynamic spin Hamiltonian adapted to each doublet. From these results and from the lifetime of the excited doublet states deduced from the EPR linewidths, five bits of experimental information on the orbit-lattice coupling have been obtained. Various models proposed for a parametrization of this coupling are tested with these results. Beside the validity of the approximations made for the building up of these models, other possibilities can explain their incompatibility with the experiments: (i) local changes in the elastic constants; (ii) existence of displacements in the strained crystal which are not predicted by the elasticity but are due to the particularity of the crystal structure. Relaxation-time measurements have also been made and some comments on their correlation with uniaxial-stress results and lifetimes are given.

I. INTRODUCTION

Crystal-field theory has been a very powerful method for spectroscopists essentially because it leads to an effective Hamiltonian with few "to determine" parameters. One of the best successes of this theory was the interpretation of the optical spectra of lanthanides for which the parameters were considerably overdetermined by the experimental results. On the other hand, *ab initio* calculations have not been as conclusive as one could hope. However, a recent model developed by Newman and his co-workers seems to lead to better results (see the review given by Newman[1]).

The dynamic coupling between an ion and its surroundings can also be analyzed within the crystal-field theory. But the number of the parameters needed for a complete description depends on the assumptions. For instance, with O_h point symmetry, this number is 7 (11 if the coupling with Γ_{1g} and Γ_{4g} modes is included) if one supposes either that the interaction is only with the ligands or that the strain is uniform around the ion.[2,3] Newman and his colleagues,[1] supposing that the major part of the interaction is due to overlap and covalency with the ligands, reduce this number to 4 (see Baker and Van Ormondt[4] for more details). Buisson and Borg,[5] using an electrostatic model and the long-wavelength approximation show that three parameters would be sufficient.

Baker and Van Ormondt[4] have recently tried to test these various models with their uniaxial-stress experiments on Tm^{2+} and Yb^{3+} in CaF_2, SrF_2, BaF_2. However, the number of bits of experimental information is only 2 for each system, and it seems difficult to relate the results obtained with different systems. Baker and Currel[6] have studied, also by uniaxial-stress experiments, the Γ_8 quadruplet of Dy^{3+} in CaF_2 and of Er^{3+} in MgO. The amount of independent experimental information is larger in these cases and the analysis of these results will be very interesting. Ho^{2+} in $SrCl_2$ is also an attractive system with O_h symmetry. After the EPR studies of Sabisky[7] and the optical measurements of Weakliem and Kiss,[8] we know that the three lower crystal-field multiplets are only split by 30 cm^{-1}, EPR experiments being possible within the two lower doublets. Thus EPR under uniaxial static stress on these doublets, measurements of direct and Orbach relaxation rates for the ground doublet, and lifetime broadening of the various lines will give a great number of independent experimental results. The frequency of the phonons involved, even for the Orbach process, is sufficiently low to permit the use of the long-wavelength approximation. While this system has the advantage of having narrow EPR lines, it presents two difficulties: (i) the high hygroscopy of the crystals and (ii) the strong hyperfine coupling of Ho^{2+}. The former was only an experimental problem. The consequence of the latter was a strong complication in the calculations. It was possible to overcome this complication in calculating the shifts induced by uniaxial static stress, but not in evaluating the relaxation rates.

In Sec. II, we give the theoretical evaluation of the line shifts induced by uniaxial static stress using an effective dynamic Hamiltonian. The experimental results of EPR under static stress, of relaxation-time measurements, and of some complementary spectroscopy measurements are given in Sec. III, and Sec. IV is devoted to a discussion

of the results.

II. THEORETICAL CONSIDERATIONS

We shall use the orbit-lattice Hamiltonian obtained in previous work[3] which supposes a uniform distortion of the lattice around the paramagnetic ion. In the case of O_h point symmetry, this Hamiltonian can be written

$$\mathcal{H}_{OL} = \sum_{l,\alpha,\beta} V(l,\Gamma_\alpha)\, s_l\, O_J(l,\Gamma_\alpha^*,\beta)\,\sigma(\Gamma_\alpha,\beta)\,. \quad (1)$$

$O_J(l,\Gamma_\alpha,\beta)$ is the J operator associated with the normalized linear combination $Y(l,\Gamma_\alpha,\beta)$ of spherical harmonics belonging to the β component of the representation Γ_α of the O_h group ($\Gamma_\alpha = \Gamma_{1g}, \Gamma_{3g}, \Gamma_{4g}, \Gamma_{5g}$), s_l are the secularization constants of Stevens, $\sigma(\Gamma_\alpha,\beta)$ the normalized linear combinations of the Cartesian components of the tensor $\sigma_{uv} = \partial(\Delta r)_u/\partial r_v^0$ [which can also be defined by $(\Delta r)_u = r_u - r_u^0 = \sum_v \sigma_{uv} r_v^0$] describing the lattice distortion (see Appendix A), and $V(l,\Gamma_\alpha)$, the parameters specific to each situation. There are 11 parameters in Eq. (1) but, as discussed in Sec. IV they can be expressed in terms of a few independent quantities, the number of which depends on the model. The $\sigma(\Gamma_\alpha,\beta)$ components are either related to the static uniaxial stress applied to the crystal for the calculation of the induced shifts or expressed in terms of phonon operators for relaxation studies.

The system studied in this work is a Kramers system having levels associated with cubic doublets Γ_6 and Γ_7 and cubic quadruplets Γ_8. As $\mathcal{H}_{OL}$ is even by time reversal, its matrix elements inside doublets are zero. However, the Zeeman interaction mixes the states of the doublets with those of the quadruplets, making these matrix elements nonzero. The hyperfine coupling can also mix the states. Abragam *et al.*[9] have studied this last effect when the hyperfine coupling is small compared to the Zeeman interaction. We shall obtain more general results which will be applied to the case of Ho^{2+}, which has a strong hyperfine coupling.

The Zeeman and hyperfine Hamiltonians are written as

$$\mathcal{H}_1 = g_J\,\mu_B\,\vec{H}\cdot\vec{J} + a\vec{I}\cdot\vec{J}\,, \quad (2)$$

where the Zeeman nuclear term $g_n\,\mu_N\,\vec{H}\cdot\vec{I}$, although of great importance for the spectroscopist, has not been included. Our problem is then to calculate the combined effect of $\mathcal{H}_1$ and $\mathcal{H}_{OL}$ on the cubic states. At the first order in perturbation theory, only $\mathcal{H}_1$ has to be considered. As usual, the result can be expressed, for the doublet Γ_i, with the spin Hamiltonian

$$\mathcal{H}_{S_i} = g_i\,\mu_B\,\vec{H}\cdot\vec{S} + A_i\,\vec{I}\cdot\vec{S}\,, \quad (3)$$

with $S = \frac{1}{2}$,

$$g_i/g_J = A_i/a = 2\langle\Gamma_i+|J_z|\Gamma_i+\rangle\,,$$

$|\Gamma_i+\rangle$ being the state $|S_z=\frac{1}{2}\rangle$ written in terms of m_J. Let $\|\Gamma_i, m, M\rangle$ ($m = m_s = \pm\frac{1}{2}$, $M = m_I$) be the eigenstates of (3) and $|\Gamma_i, m_J, m_I\rangle$, abbreviated by $|\Gamma_i, n\rangle$, the basis in which $\mathcal{H}_1$ is diagonal within each cubic multiplet Γ_i. This last basis, which corresponds to the states $\|\Gamma_i, m, M\rangle$ for the doublets, is the best for second-order calculations. At this order, $\mathcal{H}_{OL}$ must be included, and we get for the shift of the level $|\Gamma_i, n\rangle$,

$$\begin{aligned}\Delta E(\Gamma_i,n) = \sum_{j,n'} \Big(& |\langle\Gamma_i,n|\mathcal{H}_1|\Gamma_j,n'\rangle|^2 \\ & + \langle\Gamma_i,n|\mathcal{H}_1|\Gamma_j,n'\rangle\langle\Gamma_j,n'|\mathcal{H}_{OL}|\Gamma_i,n\rangle \\ & + \langle\Gamma_i,n|\mathcal{H}_{OL}|\Gamma_j,n'\rangle\langle\Gamma_j,n'|\mathcal{H}_1|\Gamma_i,n\rangle \\ & + |\langle\Gamma_i,n|\mathcal{H}_{OL}|\Gamma_j,n'\rangle|^2\Big)\frac{1}{E(\Gamma_i)-E(\Gamma_j)}\,. \end{aligned} \quad (4)$$

The first term gives the spectroscopic corrections and will be discussed in Sec. III. As $\mathcal{H}_{OL}$ is even by time reversal, the shift given by the last term is the same for all levels of each cubic doublet and cannot be observed in our experiments. The only terms to be retained are thus the central ones. Except when the magnetic field is in a special direction, the calculation is tedious and it is preferable to use an effective Hamiltonian appropriate to each cubic doublet.

The general form for such an effective Hamiltonian is well known.[9] It does not depend on the doublet, although the values of the coefficients do. We shall write it as

$$\begin{aligned}\mathcal{H}_{eff} = & g_J\,\mu_B \sum_{\alpha,\beta} A_\alpha\, C_{\alpha,\beta}(\vec{H},\vec{S})\,\sigma(\Gamma_\alpha,\beta) \\ & + a \sum_{\alpha,\beta} A_\alpha C_{\alpha,\beta}(\vec{I},\vec{S})\,\sigma(\Gamma_\alpha,\beta)\,, \end{aligned} \quad (5)$$

where $C_{\alpha,\beta}(\vec{U},\vec{V}) = \sum_{i,j}\lambda_{ij}^{\alpha\beta} U_i V_j$ is the bilinear combination of the components $U_i V_j$ which belong to the β component of Γ_α. They are, for the O_h group, when one uses the standard real form for the representations Γ_{4g} and Γ_{5g}

$$\begin{aligned} C_{3,\theta} &= \frac{1}{\sqrt{6}}(3U_zV_z - \vec{U}\cdot\vec{V}), & C_{3,\epsilon} &= \frac{1}{\sqrt{2}}(U_xV_x - U_yV_y), \\ C_{4,x} &= \frac{1}{\sqrt{2}}(U_yV_z - U_zV_y), & C_{4,y} &= \frac{1}{\sqrt{2}}(U_zV_x - U_xV_z), \end{aligned} \quad (6)$$

$$\begin{aligned} C_{4,z} &= \frac{1}{\sqrt{2}}(U_xV_y - U_yV_x), & C_{5,yz} &= \frac{1}{\sqrt{2}}(U_yV_z + U_zV_y), \\ C_{5,xz} &= \frac{1}{\sqrt{2}}(U_zV_x + U_xV_z), & C_{5,xy} &= \frac{1}{\sqrt{2}}(U_xV_y + U_yV_x). \end{aligned}$$

The number A_α, the same in the two terms because the mixing is produced by $g_J\vec{H}\cdot\vec{J}$ and $a\vec{I}\cdot\vec{J}$,

can be found by equating for some simple cases the results obtained by direct calculation with those obtained using this effective Hamiltonian, i.e., writing

$$\sum_{\Gamma_j,n'} \frac{\langle \Gamma_i,n|\mathcal{H}_1|\Gamma_j,n'\rangle\langle\Gamma_j,n'|\mathcal{H}_{OL}|\Gamma_i,n\rangle+\langle\Gamma_i,n|\mathcal{H}_{OL}|\Gamma_j,n'\rangle\langle\Gamma_j,n'|\mathcal{H}_1|\Gamma_i,n\rangle}{E(\Gamma_i)-E(\Gamma_j)} = \langle \Gamma_i,m,M\|\mathcal{H}_{eff}^{(i)}\|\Gamma_i,m,M\rangle, \tag{7}$$

where $\mathcal{H}_{eff}^{(i)}$ is the effective Hamiltonian appropriate to the doublet Γ_i.

The difficulty in the calculation lies in the fact that the states $\|\Gamma_i,m,M\rangle$ depend on the magnetic field orientation. We shall see that the knowledge of the eigenstates for $\vec{H}$ parallel to [001], which we shall denote by $\|\Gamma_i,m,M\rangle\rangle$, is sufficient. These states can easily be obtained by solving Eq. (3), and they can be written in terms of the basis $|m,M\rangle = |m\rangle|M\rangle$

$$\|m,M\rangle\rangle = \sum_{m',M'} C_{m'M'}^{mM}|m',M'\rangle ,$$

where the only nonzero $C_{m'M'}^{mM}$ coefficients are those for which $m+M=m'+M'$. The index i, referring to a specific doublet, is not indicated hereafter to simplify the notation. If the magnetic field is rotated from the z direction by a rotation $\mathcal{R}$, the eigenstates become

$$\|mM\rangle = \sum_{m',m'',M',M''} C_{m'M'}^{mM} d_{m''m'}(\mathcal{R})\mathfrak{D}_{M''M'} \times(\mathcal{R})|m'',M''\rangle ,$$

where $d(\mathcal{R})$ and $\mathfrak{D}(\mathcal{R})$ are the usual transformation matrices of electron and nuclear states under the rotation $\mathcal{R}$. The matrix elements of $\mathcal{H}_{eff}$ are

$$\begin{aligned}\langle m_1,M_1\|\mathcal{H}_{eff}\|m,M\rangle &= \sum C_{m'M'}^{mM}(C_{m_1'M_1'}^{m_1M_1})^*\langle m_1'M_1'|d^{-1}\mathfrak{D}^{-1}\mathcal{H}_{eff}\mathfrak{D}\,d|m'M'\rangle \\ &= \sum C_{m'M'}^{mM}(C_{m_1'M_1'}^{m_1M_1})^*\langle m_1'M_1'|\tilde{\mathcal{H}}_{eff}|m'M'\rangle ,\end{aligned} \tag{8}$$

where $\tilde{\mathcal{H}}_{eff}$ is the effective Hamiltonian "rotated" by $\mathcal{R}$. This Hamiltonian can be written in terms of the components of $\vec{S}$ and $\vec{I}$ whose matrix elements are simple in the basis $|m,M\rangle$. This transformation is given in Appendix B and leads to

$$\begin{aligned}\tilde{\mathcal{H}}_{eff} &= g_J\mu_B H\sum_{\alpha,\beta} A_\alpha B_i^{\alpha\beta}S_i\,\sigma(\Gamma_\alpha,\beta) \\ &+ a\sum_{\substack{\alpha,\beta\\ i,j}} A_\alpha T_{ij}^{\alpha\beta}I_iS_j\sigma(\Gamma_\alpha,\beta) ,\end{aligned} \tag{9}$$

where the matrices $B^{\alpha\beta}$ and $T^{\alpha\beta}$, which depend only on the rotation $\mathcal{R}$ are given in Appendix B.

Equation (9) is a generalization of the results obtained by Abragam *et al.*[9] in the case of a hyperfine interaction small compared to the Zeeman effect. From this equation one can calculate the shifts induced by uniaxial stress or the transition probabilities due to the phonons. We begin with the shifts which involve only the diagonal matrix elements

$$\begin{aligned}\langle m,M\|\mathcal{H}_{eff}\|m,M\rangle &= \sum C_{m'M'}^{mM}(C_{m_1'M_1'}^{mM})^*\langle m_1'M_1'|\tilde{\mathcal{H}}_{eff}|m'M'\rangle .\end{aligned}$$

In this equation, we keep only the Γ_{3g} and Γ_{5g} parts of $\mathcal{H}_{eff}$ since a uniaxial stress cannot induce the Γ_{4g} "rotations".

As the $C_{m'M'}^{mM}$ are nonzero only if $m+M=m'+M'$, the number of matrix elements we have to calculate is not too large. For the first part of $\tilde{\mathcal{H}}_{eff}$, which originates in the Zeeman term, $M_1'=M'$ and $m_1'=m'$; thus only the S_zI_z terms have to be considered. The second part of $\tilde{\mathcal{H}}_{eff}$ involves two sorts of terms: (i) those with $m'=m_1'$ and $M'=M_1'$; (ii) those with $m'\neq m_1'$ and $M'\neq M_1'$, but with $m'+M'=m_1'+M_1'$. The former are calculated as the Zeeman terms, while the expression of the latter needs the calculation of I_+S_- and I_-S_+ terms of $\tilde{\mathcal{H}}_{eff}$. The final result is

$$\begin{aligned}\Delta E_{m,M} = K(m,M)\{&A_3[(3\cos^2\theta-1)\sigma(\Gamma_{3g},\theta) \\ &+\sqrt{3}\sin^2\theta\cos2\phi\,\sigma(\Gamma_{3g},\epsilon)] \\ &+\tfrac{1}{2}\sqrt{2}\,A_5\{\sin2\theta[\sigma(\Gamma_{5g},yz)\sin\phi \\ &+\sigma(\Gamma_{5g},xz)\cos\phi]+\sin^2\theta\sin2\phi\,\sigma(\Gamma_{5g},xy)\}\},\end{aligned} \tag{10}$$

with

$$\begin{aligned}K(m,M) = \tfrac{1}{2}g_J\mu_BH(&|C_{1/2}^{mM}|^2-|C_{-1/2}^{mM}|^2) \\ &+\tfrac{1}{2}a[(m+M-\tfrac{1}{2})|C_{1/2}^{mM}|^2-(m+M+\tfrac{1}{2})|C_{-1/2}^{mM}|^2 \\ &-C_{-1/2}^{mM}C_{1/2}^{mM}\langle m+M+\tfrac{1}{2}|I_+|m+M-\tfrac{1}{2}\rangle] .\end{aligned}$$

This result is relatively simple. It shows that the angular dependance is the same for the two parts of $\tilde{\mathcal{H}}_{eff}$. The shifts given by[10] are those of the levels of any cubic doublet, the values of $K(m,M)$, A_3, and A_5 being determined in each case by using the spin Hamiltonian (3) and Eq. (7), respectively. In the case of Ho^{2+} in $SrCl_2$, we can observe the shifts inside two doublets Γ_7 and Γ_6. The corresponding values for the A's are, ignoring Γ_8^2 and Γ_8^3 levels

$$A_3^i = \frac{2\langle \Gamma_i, -\frac{1}{2}|J_z|i, \Gamma_8, -\frac{1}{2}\rangle}{E(\Gamma_i)-E(\Gamma_8)} B_i(\Gamma_{3g}, \theta),$$
$$A_5^i = -\frac{\langle \Gamma_i, \frac{1}{2}|J_-|i, \Gamma_8, \frac{3}{2}\rangle}{E(\Gamma_i)-E(\Gamma_8)} B_i(\Gamma_{5g}, 0) \quad (i = 7, 6), \tag{11}$$

where $|i, \Gamma_8, m\rangle$ $(m = \pm\frac{1}{2}, \pm\frac{3}{2})$ is the basis for the Γ_8 multiplet which is such that

$$\langle \Gamma_i, m|J_z|j, \Gamma_8, m\rangle \neq 0 \quad \text{only if} \quad i = j \quad (m = \pm\tfrac{1}{2}),$$

and the $B_i(\Gamma_\alpha, \beta)$ are defined by

$$B_i(\Gamma_{3g}, \theta) = \sum_l s_l \langle i, \Gamma_8, -\tfrac{1}{2}|V(l, \Gamma_{3g}) \times O(l, \Gamma_{3g}, \theta)|\Gamma_i, -\tfrac{1}{2}\rangle,$$
$$B_i(\Gamma_{5g}, 0) = \sum_l s_l \langle i, \Gamma_8, \tfrac{3}{2}|V(l, \Gamma_{5g}) \times O(l, \Gamma_{5g}, 0)|\Gamma_i, -\tfrac{1}{2}\rangle. \tag{12}$$

The problem of finding the relaxation time due to the direct process is more complex. First, we must evaluate all the matrix elements of $\mathcal{H}_{eff}$ between the 16 states of each doublet. This is easy in principle using Eqs. (8) and (9), but very tedious. Bernstein and Franceschetti[10] have recently made this calculation for Ho^{2+} in CaF_2. Second, we must solve the system of 16 rate equations in order to get the evolution of the populations after the equilibrium has been destroyed. As the various transition probabilities are of the same order of magnitude for reasonable magnetic field, there is no simple way to solve this system as was the case for Tm^{2+} in CaF_2.[9] We have not tried to overcome this problem.

III. EXPERIMENTAL RESULTS

A. Samples and apparatus

The $SrCl_2$-doped crystals studied were obtained from the Advanced Technology Center, Inc. of Dallas, from Bill, and from Chapelle. Most of the uniaxial stress results were obtained with those provided by Chapelle because their very good quality allowed higher pressures to be used. All the crystals were received with the holmium in the trivalent state. The conversion to Ho^{2+} was achieved by the well known technique of solid electrolysis.[11,12] For the uniaxial stress experiments, the samples were cut as cylinders with axes parallel to the ⟨100⟩, ⟨110⟩, and ⟨111⟩ directions, respectively.

The experimental arrangement was described in a previous paper.[13] It consists of a cylindrical X-band cavity with an adjustable coupling and a mechanical system to apply the stress to the crystal. This system comprises a stainless-steel rod which transmits the compression via a steel sphere to a sandwich consisting of the specimen placed between two quartz cylinders whose faces are well polished. Under pressure, the system is self aligning and a good homogeneity of stress in the sample is obtained. In order to maintain a leak-tight system, the stainless-steel rod was operated through a bellows at the head of the cryostat. This arrangement lowered the effect of solid friction on the transmission of the applied force. This force is vertical, and the magnetic field can be orientated in any direction in the horizontal plane.

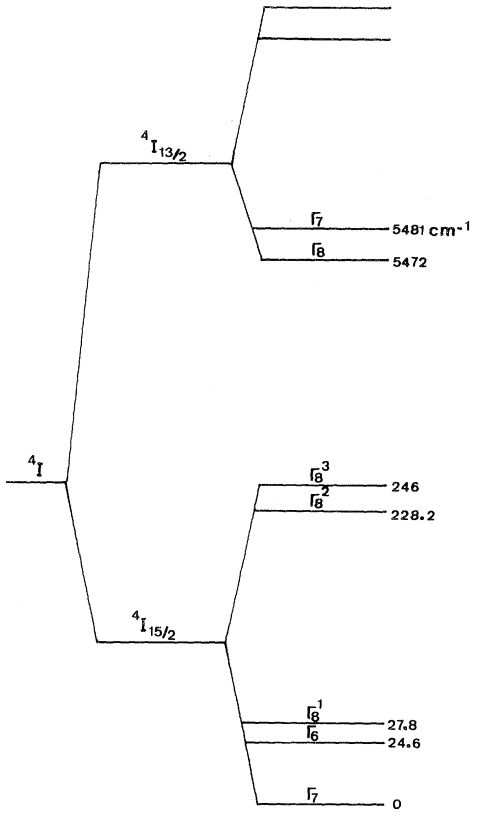

FIG. 1. Crystal-field splitting of the $^4I_{15/2}$ and $^4I_{13/2}$ levels of Ho^{2+} in $SrCl_2$ from optical spectroscopy (Ref. 8).

B. Remarks on the spectroscopy

The $^4I_{15/2}$ ground term of the Ho^{2+} ion is split by the cubic crystal field into various multiplets, as shown in Fig. 1. The strong hyperfine coupling and the applied magnetic field lift the degeneracy of these multiplets. Figure 2 shows the levels for the ground Γ_7 doublet. The EPR of this doublet has been studied in great detail by Sabisky[7] and Szofran *et al.*[14] They have shown that the simple form (3) for the spin Hamiltonian is not sufficient for the interpretation of the spectra. Second-order contributions of Hamiltonian (2), as expressed by the first term of Eq. (4), must be included. They give additional terms in the spin Hamiltonian. The spectra observed at 870 MHz (Szofran *et al.*), at 9000 MHz

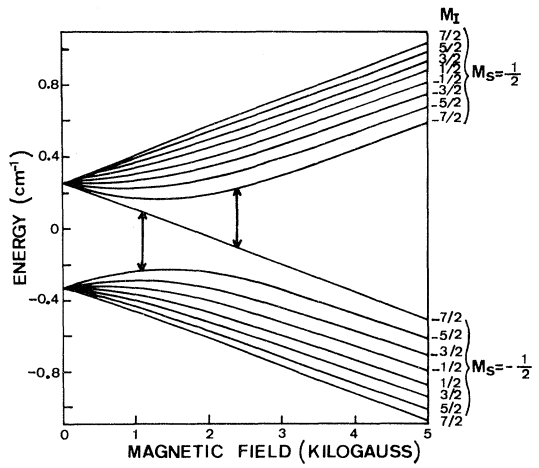

FIG. 2. Energy levels of the ground Γ_7 doublet as a function of the magnetic field. The arrows show the two transitions observed at 9300 Mhz, the low-field line and the high-field line.

(Sabisky and this work), at 27000 MHz (Sabisky), and at 36000 MHz (this work) can be interpreted with

$$\mathcal{H}=g\mu_B \vec{H}\cdot\vec{S}+A\vec{I}\cdot\vec{S}-g_n'\beta_n\vec{H}\cdot\vec{I}\ , \qquad (13)$$

with $S=\frac{1}{2}$, $I=\frac{7}{2}$, $g=6.751$, $A=0.1478$ cm^{-1}, and $g_n'=46\pm3$.

The detailed study of the resonance in the Γ_6 excited doublet is less easy because the lines are broader and of lower intensity. The levels have a disposition analogous to those of Γ_7 (see Fig. 2), but the negative signs of g and A make the level $|-\frac{1}{2},\frac{7}{2}\rangle$ the highest and the $|\frac{1}{2},\frac{7}{2}\rangle$ the lowest. The nearly isotropic spectrum observed at 9000 MHz by Sabisky and ourselves can be interpreted by the spin Hamiltonian (13) with $S=\frac{1}{2}$, $I=\frac{7}{2}$, $g=-5.91$, $A=-0.133$ cm^{-1}, and $g_n'=420\pm30$, the large value of g_n' being a result of the proximity of the Γ_8 quadruplet. Weakliem and Kiss (8) have studied the optical spectroscopy of Ho^{2+} in $SrCl_2$. Their results give the position of the various crystal-field levels indicated in Fig. 1. One can then deduce the values of the parameter x and of the energy scale W introduced by Lea, Leask, and Wolf:[15]

$$x=-0.396\ , \qquad W=0.739\ \text{cm}^{-1}\ .$$

We can thus use the eigenstates tabulated in this reference for $x=-0.4$. If we write the static-crystal-field Hamiltonian as

$$\mathcal{H}_s=\sum_{l=4,6}A(l,\Gamma_{1g})s_l O_J(l,\Gamma_{1g})\ ,$$

with the same definition for s_l and $O_J(l,\Gamma_{1g})$ as for $\mathcal{H}_{OL}$ in Eq. (1), we obtain, for the static-crystal-field parameters,

$$A(4,\Gamma_{1g})=-1360\ \text{cm}^{-1}\ , \quad A(6,\Gamma_{1g})=692\ \text{cm}^{-1}\ . \qquad (14)$$

C. Uniaxial-stress results

Because of the strong hyperfine coupling, it is only possible to observe two lines for each doublet at X band. We shall label $\Gamma_{i,HF}$ and $\Gamma_{i,LF}$ ($i=7,6$) the high-field and the low-field lines, respectively, for each doublet (see Fig. 2). Although the signs of g and A are opposite for the two doublets, the $\Gamma_{i,HF}$ lines are associated with the transitions $\|\Gamma_i,\frac{1}{2},-\frac{7}{2}\rangle\leftrightarrow\|\Gamma_i,-\frac{1}{2},-\frac{7}{2}\rangle$ and the $\Gamma_{i,LF}$ lines to the transitions $\|\Gamma_i,-\frac{1}{2},-\frac{7}{2}\rangle\leftrightarrow\|\Gamma_i,-\frac{1}{2},-\frac{5}{2}\rangle$, what ever the doublet concerned.

The influence of the stress on the position of the lines is illustrated in Fig. 3. The shifts of the Γ_6 lines are enhanced owing to the proximity of the Γ_8 multiplet, and thus, fortunately, the great width of these lines does not mask the shift. The non-broadening of the lines when the force is applied is an indication of the good uniformity of the strains inside the sample.

The results of systematic measurements of the shifts of the lines are given in Figs. 4 and 5. Except for very small forces, the shifts are linearly related to the applied force. The origin of the apparent nonlinearity at low stress is certainly due to some residual solid friction in the apparatus. When the force is applied along a $\langle100\rangle$ or a $\langle111\rangle$ direction, the shifts are isotropic and are given by

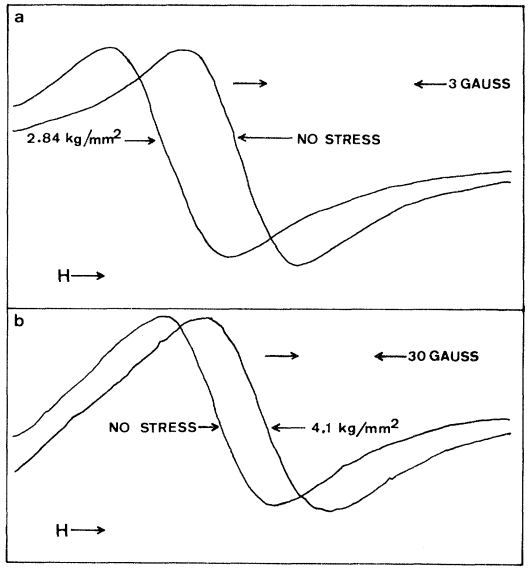

FIG. 3. Typical results showing the uniaxial induced shift. (a): High-field line Γ_7 with the force along the [111] direction; (b): High-field line Γ_6 with the force along the [110] direction and the field along the [001] direction.

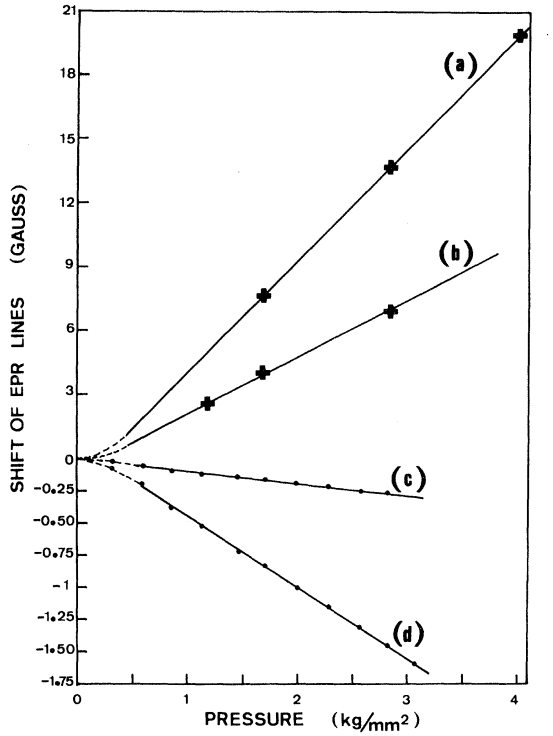

FIG. 4. Dependence of the shifts versus the applied stress. (a): High-field Γ_6 line with $\vec{P} \| [110]$ and $\vec{H} \| [001]$; (b): High-field Γ_6 line with $\vec{P} \| [111]$; (c): Low-field Γ_7 line with $\vec{P} \| [100]$; (d): High-field Γ_7 line with $\vec{P} \| [111]$.

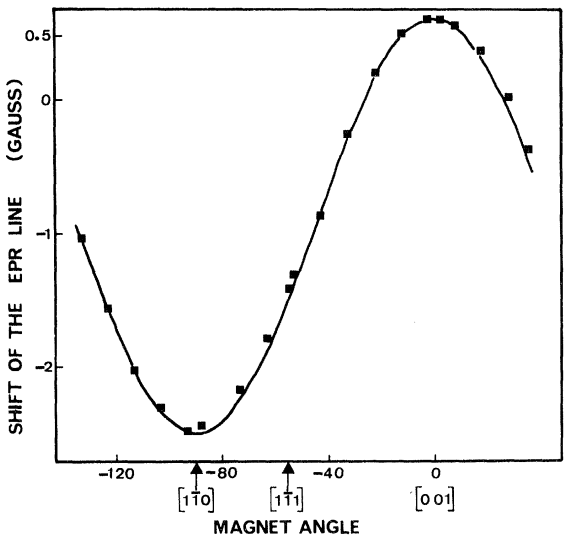

FIG. 5. Angular dependence of the shift for the high-field Γ_7 line, The stress of about 250 kg/cm^2 is along the [110] direction: the magnetic field lies in the (110) plane. The points are experimental, the curve is the theoretical variation deduced from Eq. (10) (see Sec. IV A).

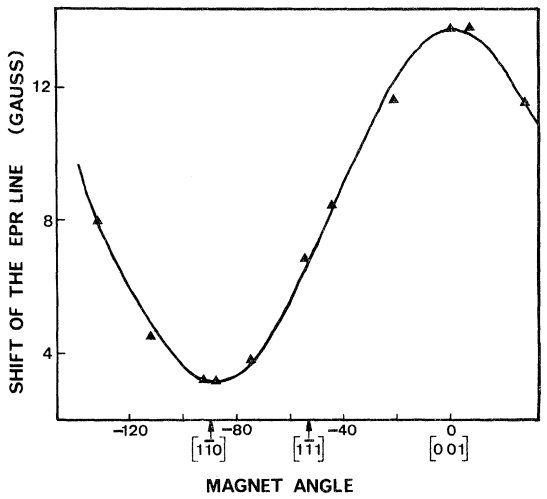

FIG. 6. Angular dependence of the shift for the high-field Γ_6 line. The stress of about 250 kg/cm^2 is along the [110] direction; the magnetic field lies in the (110) plane. The points are experimental: the curve is the theoretical variation deduced from Eq. (10) (see Sec. IV A).

$$
\begin{aligned}
(\Delta H/\Delta P_{\langle 111\rangle})\Gamma_{7HF} &= -5.5\times 10^{-3}\ \mathrm{G\,cm^2/kg}\ , \\
(\Delta H/\Delta P_{\langle 001\rangle})\Gamma_{7HF} &= 2.2\times 10^{-3}\ \mathrm{G\,cm^2/kg}\ , \\
(\Delta H/\Delta P_{\langle 111\rangle})\Gamma_{7LF} &= 2.4\times 10^{-3}\ \mathrm{G\,cm^2/kg}\ , \\
(\Delta H/\Delta P_{\langle 001\rangle})\Gamma_{7LF} &= -0.96\times 10^{-3}\ \mathrm{G\,cm^2/kg}\ .
\end{aligned}
\tag{15}
$$

When the force is along a $\langle 110\rangle$ axis, the shift depends on the magnetic field orientation. The results for the high-field line are given on Fig. 5.

The measurements on the Γ_6 lines are less easy owing to the weak intensity and the width of these lines; we have thus fewer results than for the Γ_7 lines. Figure 4 shows that the variation of the shift with the applied stress is again linear. The near Γ_8 quadruplet creates a weak anisotropy for the lines in the unstressed crystal which is nevertheless bigger than the shifts induced by the applied force. The shifts themselves remain isotropic when the force is parallel to a $\langle 100\rangle$ or a $\langle 111\rangle$ axis. We find

$$
\begin{aligned}
(\Delta H/\Delta P_{\langle 100\rangle})\Gamma_{6HF} &= 5.55\times 10^{-2}\ \mathrm{G\,cm^2/kg}\ , \\
(\Delta H/\Delta P_{\langle 111\rangle})\Gamma_{6HF} &= 2.6\times 10^{-2}\ \mathrm{G\,cm^2/kg}\ , \\
(\Delta H/\Delta P_{\langle 111\rangle})\Gamma_{6LF} &= -1.6\times 10^{-2}\ \mathrm{G\,cm^2/kg}\ .
\end{aligned}
\tag{16}
$$

The angular variation when the force is along a $\langle 110\rangle$ axis is shown in Fig. 6.

D. Relaxation-time measurements

We have measured the T_1 of the Γ_7 ground doublet lines in liquid-helium temperature range at X-band

frequency with an apparatus previously described.[13] The results obtained for the low-field line are shown in Fig. 7. They can be fitted by

$$1/T_1 = (76 \pm 2)T + (1.25 \pm 0.2) \times 10^9 e^{-35.4/T} + (4.5 \pm 0.3) \times 10^{10} e^{-40/T}, \quad (17)$$

for the low-field line. For the high-field line the result is the same except for the direct process which goes as $61T$. We must point out that for this fitting we have left fixed the values of the arguments of the exponential since we know the position of the excited levels. There is a great margin of error for the coefficients because the arguments are not very different. It is even possible to have a good fit with only one exponential term, the value of the argument being interdemediary between the previous ones.

E. Linewidth measurements

The linewidths had previously been measured by Sabisky.[7] We have only verified his results for a few temperatures. Figure 8 gives Sabisky's results for the variation of the full-width-at-half-maximum amplitude. We have decuded the transverse relaxation time T_2 from these results using a procedure described elsewhere,[16] in which the line is supposed to be the convolution of Gaussian and Lorentzian distributions. The former describes the low-temperature linewidth, the latter the effect of the lifetime of the states which vary with temperature. The corresponding points are also plotted in Fig. 7. They can be fitted by

$$1/T_2 = 1.34 \times 10^9 (e^{35.4/T} - 1)^{-1} + (9.5 \pm 0.5) \times 10^{10} (e^{40/T} - 1)^{-1}, \quad (18)$$

where the value 1.34×10^9 is deduced from the Γ_6 linewidth and left fixed for the fitting. The problem of the relation between T_1 and T_2, recently discussed by Stapleton and his colleagues[17,18] for other systems, will be commented upon in Sec. IV H.

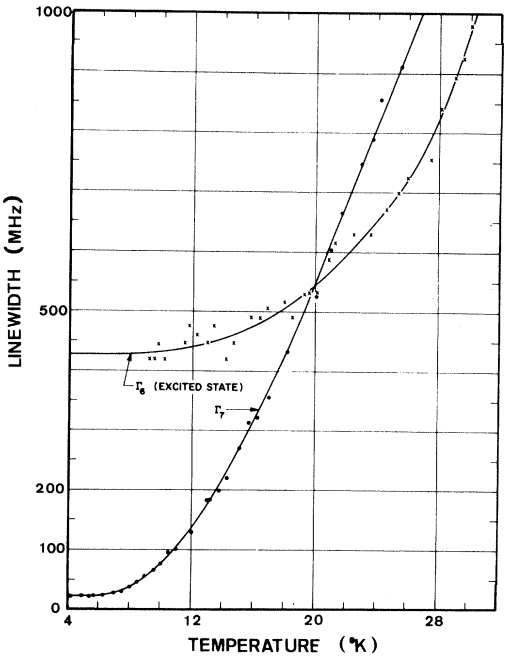

FIG. 8. Temperature dependence of the full linewidth at half-height for the Γ_6 and Γ_7 lines (from Sabisky's thesis).

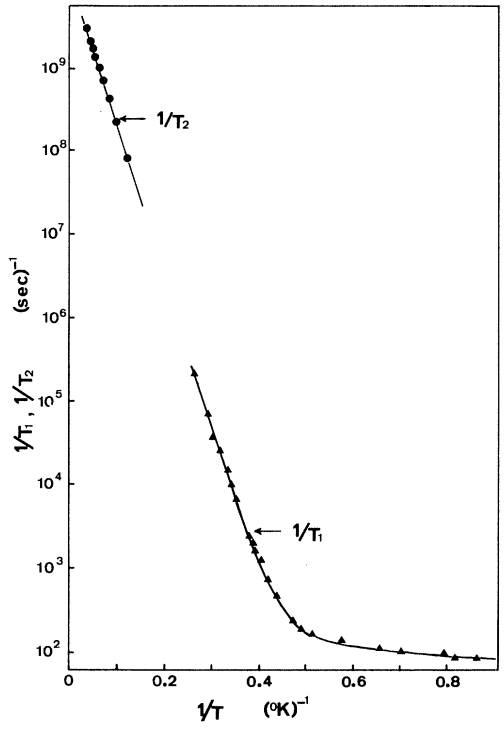

FIG. 7. Temperature dependence of the relaxation times T_1 and T_2 for the Γ_7 low-field line. The triangles are the experimental values of $1/T_1$ obtained from saturation-recovery technique. The full circles are the values of $1/T_2$ deduced from the linewidth given in Fig. 8. The two curves represent Eqs. (17) and (18).

IV. DISCUSSION

A. Consistency of the experimental results

Formula (10) of Sec. II enables the angular variation of the shift when the force is applied along a ⟨110⟩ direction to be predicted in terms of the shifts observed for a particular stress orientation. We have plotted in Figs. 5 and 6 the curves showing this theoretical variation using the experimental values given by Eqs. (15) and (16). From formula (10), we can also show that for any direction of the applied force

$$\left(\frac{\Delta H}{\Delta P}\right)_{HF} \Big/ \left(\frac{\Delta H}{\Delta P}\right)_{LF} = \begin{cases} -2.31 & \text{for } \Gamma_7 \text{ lines} \\ -1.61 & \text{for } \Gamma_6 \text{ lines} . \end{cases}$$

The experimental values of these ratios are, respectively, -2.3 ± 0.05 and -1.6 ± 0.05. The good agreement both for these ratios and for the angular dependence together with the linear variation of the shift with respect to the stress shows the validity of the hypothesis made in Sec. II, i.e., neglect of terms higher than 2 in perturbation theory.

B. Values of the dynamic-spin-Hamiltonian parameters

The A_α^i values of Eq. (11) can be deduced from our experimental results if we express the strains $\sigma(\Gamma_\alpha, \beta)$ as a function of the applied force by using the elastic constants. Lauer *et al.*[19] have measured the elastic constants by an ultrasonic method between 300 and 195 °K. By extrapolation of their results to helium temperature with the same law as that found by Huffman *et al.*[20] for CaF_2, we deduce

$$C_{11} - C_{12} = 5.58 \times 10^{11} \text{ dyn/cm}^2 ,$$

$$C_{44} = 1 \times 10^{11} \text{ dyn/cm}^2 .$$

Other measurements,[21] based on Brillouin scattering experiments, have given

$$C_{11} - C_{12} = 5.14 \times 10^{11} \text{ dyn/cm}^2 ,$$

$$C_{44} = 0.8 \times 10^{11} \text{ dyn/cm}^2 .$$

Using the average values of these two results, and $g_J = \frac{6}{5}$, $a = 0.0261 \text{ cm}^{-1}$, we deduce

$$A_3^7 = -26.7 , \qquad A_5^7 = -19.6 ,$$

$$A_3^6 = 357 , \qquad A_5^6 = 49.1 .$$

C. Equations for the determination of the orbit-lattice parameters

With these values for the A's, Eqs. (11) and (12) can be written in numerical form once the matrix elements of the operators O_J are calculated. As pointed out in Sec. III B, we use for this calculation the states of Lea, Leask, and Wolf[15] for $x = -0.4$. The result is

$$B_7(\Gamma_{3g}, \theta) = [-2.03\, V(2, \Gamma_{3g}) - 1.684\, V(4, \Gamma_{3g}) + 2.34\, V(6, \Gamma_{3g})] \times 10^{-2} = -117 \text{ cm}^{-1} , \tag{19a}$$

$$B_7(\Gamma_{5g}, 0) = [-3.372 V(2, \Gamma_{5g}) + 1.51 V(4, \Gamma_{5g}) - 8.392 V(6, \Gamma_{5g}, a) - 3.759 V(6, \Gamma_{5g}, b)] \times 10^{-2} = -98 \text{ cm}^{-1} , \tag{19b}$$

$$B_6(\Gamma_{3g}, \theta) = [-5.323 V(2, \Gamma_{3g}) + 0.532 V(4, \Gamma_{3g}) - 13.183 V(6, \Gamma_{3g})] \times 10^{-2} = -137 \text{ cm}^{-1} , \tag{19c}$$

$$B_6(\Gamma_{5g}, 0) = [-0.55 V(2, \Gamma_{5g}) + 2.371 V(4, \Gamma_{5g}) + 1.129 V(6, \Gamma_{5g}, a) - 0.387 V(6, \Gamma_{5g}, b)] \times 10^{-2} = -23 \text{ cm}^{-1} , \tag{19d}$$

where the $V(\ell, \Gamma_\alpha)$ are expressed in cm^{-1}.

Another equation can be obtained by expressing the width of the Γ_6 lines at zero temperature. For this calculation we can, as a first approximation, ignore the hyperfine structure and equate the width $\Delta\omega$ to the sum of transition probabilities from the two Γ_6 levels to the two Γ_7 levels. These transition probabilities involve only strains of the Γ_{5g} type. The result is

$$\Delta\omega = \mathfrak{a}\, 6 M^2 (\Delta_6 / \hbar)^3 , \tag{20}$$

with $\mathfrak{a} = 1/6\pi\rho v^5 \hbar$, where ρ is the density of $SrCl_2$ (3.05 g/cm^3), v an average speed of sound, Δ_6 the splitting between Γ_6 and Γ_7 doublets, and M a matrix element of the orbit-lattice Hamiltonian expressed in terms of orbit-lattice parameters by

$$M = [-2.634 V(2, \Gamma_{5g}) + 2.3 V(4, \Gamma_{5g}) - 4.022 V(6, \Gamma_{5g}, a) - 1.04 V(6, \Gamma_{5g}, b)] \times 10^{-2} . \tag{21}$$

If we take into account the hyperfine structure, the value of $\Delta\omega$ is only slightly changed, the factor 6 being replaced by 5.3. To deduce the value of M from the experimental width, we have to evaluate the average speed v. Using the average values of the elastic constants and an averaging formula previously given,[3] we find $v = 2.98 \times 10^5$ cm/sec. Baker *et al.*[4] have made a more rigorous calculation of the coefficient $\mathfrak{a}$ by taking into account the anisotropy of the crystal. They have kindly put in their program the elastic constants of $SrCl_2$ and found that, for the Γ_{5g} modes (which are the only active ones in the lifetime of the Γ_6 levels), the average v is equal to 2.16×10^5 cm/sec (2.8×10^5 cm/sec for the Γ_{3g} modes). Thus there is a factor of 5 on $\mathfrak{a}$, i.e., $\sqrt{5}$ on M, depending on the method used for the evaluation of v. We have chosen the value obtained with the method of Baker *et al.*, which gives $|M| \simeq 60 \text{ cm}^{-1}$. By comparison with the value given by the point-charge model, we adopt the value $M = -60 \text{ cm}^{-1}$.

The five equations (19) and (21) are not sufficient to determine the values of the seven parameters $V(\ell, \Gamma_\alpha)$. To go further, we choose some particular models and study their compatibility with our results.

D. Point-charge model

The expressions for the static-crystal-field parameters and for the $V(\Gamma_\alpha, \beta)$ within the point-charge model have been given many times, unfortunately with a great variety of normalization. We shall not add the new formula resulting from the normalization adopted in writing Eq. (1), where both the $O_J(\ell, \Gamma_\alpha, \beta)$ and the $\sigma(\Gamma_\alpha, \beta)$ are normalized to unity. We have, however, verified their com-

TABLE I. Values of the crystal-field parameters within various models and of the corresponding $B_i(\Gamma_\alpha,\beta)$ and M appearing in Eqs. (19) and (21) (in cm^{-1}).

	Model I	Model II	Model III	Semiexperimental[a]
$A(4,\Gamma_{1g})$	−279	−1360	−1360	−1360
$A(6,\Gamma_{1g})$	55	692	692	692
$V(2,\Gamma_{3g})$	7090	7090	3545	6450
$V(4,\Gamma_{3g})$	617	3010	3010	−970
$V(6,\Gamma_{3g})$	−73	−912	−912	−1350
$V(2,\Gamma_{5g})$	4730	4730	2365	4270
$V(4,\Gamma_{5g})$	1270	6196	6196	923
$V(6,\Gamma_{5g},a)$	−67	−836	−836	−836
$V(6,\Gamma_{5g},b)$	−19.8	−248	−248	−597
$B_7(\Gamma_{3g},\theta)$	−156	−216	−144	−146 (−117)
$B_7(\Gamma_{5g},\theta)$	−134	+13.5	+93	−37 (−98)
$B_6(\Gamma_{3g},0)$	−364	−241	−52.5	−168 (−137)
$B_6(\Gamma_{5g},0)$	+3.4	+112	+125	−8.7 (−23)
M	−92	+54	+116	−51 (−64)

[a]We have given in this column the values of $A(4,\Gamma_{1g})$ and $A(6,\Gamma_{1g})$ deduced from optical spectroscopy results of Weakliem and Kiss (Ref. 8), the values of the $V(\ell,\Gamma_\alpha)$ obtained from our experiments within the electrostatic model described in Sec. IVF (see also Table II), the values of the $B_i(\Gamma_\alpha,\beta)$ and M of Eqs. (19) and (21) obtained with these $V(\ell,\Gamma_\alpha)$, and, in parenthesis, the values of the $B_i(\Gamma_\alpha,\beta)$ and M deduced from the experimental shifts and lifetime using the bulk elastic constants.

patibility with those previously published.[22] Taking into account the contribution of the first two shells of neighbors, we give in Table I the values obtained in the three following cases: (i) we use for the $\langle r^n\rangle$ the values quoted by Sroubek *et al.*[23] and without any screening effect; (ii) we deduce the values of $ee'\langle r^4\rangle/R^5$ and $ee'\langle r^6\rangle/R^7$, R being the ion-ligand distance, from the experimental values of $A(4,\Gamma_{1g})$ and $A(6,\Gamma_{1g})$, keeping the point-charge value for second-order terms; (iii) the same method as in (ii) but with a screening coefficient of 0.5 for the second-order terms. We can then calculate the $B_i(\Gamma_\alpha,\beta)$ and M of Eqs. (19) and (21) and compare the results with the experimental values (see Table I). It is not without interest to point out that the crudest model (I) gives the best agreement, as was found by Sroubeck *et al.*[23] in analogous systems (see Sec. IVG).

E. Newman model

Newman and his co-workers have developed a model for the crystal field which appears to explain better than the previous models the experimental values of the static crystal fields in low-symmetry systems.[1] The extension of this model to the dynamic case has been discussed by Baker *et al.*[4] The essential assumption that the major part of the ion-ligand interaction is covalent in nature. It is then sufficient to consider only the first neighbors. The number of quantities for the parametrization is reduced to four: three for the exponents of the R dependence of the terms of second, fourth, and sixth order (noted t_2, t_4, t_6) and another to characterize the influence of the second-order terms (the influence of the fourth- and sixth-order terms is related to the static-crystal-field values).

As for the Γ_{3g} strains, there is no change in the ion-ligand distance; the exponents t_l are not involved. The $V(4,\Gamma_{3g})$ and $V(6,\Gamma_{3g})$ are related to the static parameters by

$$V(4,\Gamma_{3g}) = -2\sqrt{\tfrac{10}{21}}\,A(4,\Gamma_{1g}),$$

$$V(6,\Gamma_{3g}) = -\tfrac{1}{2}\sqrt{\tfrac{21}{2}}\,A(6,\Gamma_{1g}),$$

$V(2,\Gamma_{3g})$ being a "to determine" quantity. The $A(\ell,\Gamma_{1g})$ are given by Eq. (14). Equations (19a) and (19c) give then two values for $V(2,\Gamma_{3g})$ which must be equal if the model is good. We find, in fact, 2660 and 5790 cm^{-1}, which are far from being equal. We can get equal values by choosing for $(C_{11}-C_{12})$ a value 2.1 times larger than the value for the bulk material, $V(2,\Gamma_{3g})$ then being equal to 9000 cm^{-1}. That the elastic constants could be locally modified is not surprising, but the factor of 2 seems not to be realistic (see Sec. IVG).

The three results obtained with the Γ_{5g} strains and the width of the Γ_6 lines are sufficient to calculate the three exponents t_l once the value of $V(2,\Gamma_{3g})$ is known, but in this case the validity of the model is not tested. Using for $V(2,\Gamma_{3g})$ the two values 2660 and 5790 cm^{-1}, we obtain, respectively, $t_2=4.9$, $t_4=-2.7$, and $t_6=5.2$ and $t_2=0.21$, $t_4=-4.2$, and $t_6=1.2$. Again these values are not realistic, especially the sign of t_4. As a comparison, Anderson *et al.*[24] have found that the values $t_4=t_6=12$ are in agreement with the variation of the static-crystal-field parameters of Tm^{2+} in CaF_2, SrF_2, BaF_2, while Baker *et al.*[4], after choosing $t_4=t_6=7$, obtain for t_2, with the same systems, values between 1.5 and 23, depending on the corrections for local displacements and local elastic constants they made (see Sec. IVG).

F. An electrostatic model

Buisson and Borg[5] have recently shown, using a pure electrostatic (but not point-charge) model for the interaction between the paramagnetic ion and all the lattice ions, that only three independent parameters are needed for the description of the dynamic coupling. The essential hypothesis leading to this result can be sketched as follows. All possible interactions, including overlap and exchange, being taken into account for a *self-consistent* determination of the static charge distribution (which need not be known but from which it is supposed possible to calculate formally the energy of the paramagnetic electron by pure electrostatic inter-

TABLE II. Results of the resolution of the 10 systems of equations (see Sec. IV F). A: with the experimental values appearing in the second members of Eqs. (19) and (21); B: with these values respectively multiplied by 1.25, 0.4, 1.25, 0.4, 0.82.

Equations omitted	A			B		
	$V(2,\Gamma_{3g})$	$V(4,\Gamma_{3g})$	$V(6,\Gamma_{3g})$	$V(2,\Gamma_{3g})$	$V(4,\Gamma_{3g})$	$V(6,\Gamma_{3g})$
(17a), (17b)	6446	−1426	−1623	6478	−957	−1358
(17b), (17c)	6092	−1376	−694	6463	−955	−1317
(17c), (17d)	6870	−592	545	6450	−968	−1338
(17d), (18)	6991	−4211	−1955	6450	−981	−1347
(18), (17a)	13046	−921	−4267	6498	−956	−1367
(17a), (17c)	5365	−1273	1211	6475	−957	−1349
(17c), (18)	6891	−1203	123	6449	−958	−1331
(18), (17b)	5540	−1496	−1260	6439	−960	−1342
(17b), (17d)	5691	−1779	−1333	6445	−972	−1345
(17d), (17a)	47152	−17610	−17291	6599	−901	−1404

action), the perturbation caused by an uniaxial stress can be described as a uniform deformation of this charge distribution. The weakness of this method is mostly in the neglect of the *variation* of exchange and overlap induced by the stress, although their contribution to the static crystal field is taken into account. From this model, one can obtain relations between the parameters $V(l,\Gamma_\alpha)$. Using these relations, given in Ref. 5, we can transform Eqs. (19) and (21) into five equations with only three unknowns, say $V(2,\Gamma_{3g})$, $V(4,\Gamma_{3g})$, $V(6,\Gamma_{3g})$. To study the compatibility of these equations, we have solved all of the 10 possible systems of three equations. The results are given in Table II. To improve the agreement, we have modified the values of the $B_i(\Gamma_\alpha,\beta)$ and M which are proportional to the elastic constants until the equations become compatible. We give in Table II the modifying factors and the results of solving the 10 corresponding systems. These values of the parameters $V(l,\Gamma_{3g})$ and the other ones deduced using the relations of Ref. 5 are also given in Table I, column 3, for comparison with the other models.

G. Conclusion on the various models

While the crudest model I (point charge with no shielding) gives static-crystal-field parameters in complete disagreement with the experiments, it gives values for the $B_i(\Gamma_\alpha,\beta)$ and for M which are not too far, except for $B_6(\Gamma_{5g},0)$, from the values deduced from the measurements using the bulk elastic constants (see Table I). It gives even better values than models II and III, usually considered to be more realistic. This surprising result was already observed for Ho^{2+} in CaF_2 and Yb^{3+} in ThO_2 by Sroubeck *et al.*,[23] who even obtained a very good agreement. Baker and Van Ormondt[4] get for the parameters A_3 and A_5 good or reasonable values for Yb^{3+} in CaF_2, Tm^{2+} in BaF_2, less good for Tm^{2+} in SrF_2, and in complete disagreement with experiments only for Tm^{2+} in CaF_2. Although one can find many systems for which this naive model works, it is hard to imagine that the physics is correctly described by it.

The two other models considered in Secs. IV E and IV F are not "*ab initio* models" permitting calculations of the orbit lattice parameters, but "parametrizing models" predicting some relations between various experimental observations. These relations are not verified for the system studied here, neither for one nor for the other. Before deducing any conclusion, we must discuss two complications not yet considered. The first results from the fact that the strain around the paramagnetic ion is different from the bulk strain calculated from the applied force by the elastic constants of the material. This problem of the local elastic constants has recently been reexamined by Malkin and Ivanenko in a series of papers[25] for CaF_2-type crystals doped with some rare-earth ions and by Kesharwani and Agrawal[26] for CsCl-type crystals doped with alkaline ions. The results of Malkin and Ivanenko show that $(C_{11}-C_{12})$ can be increased up to 10% and that C_{44} can be modified by a factor between 1.35 and 0.88, depending on the crystal and the ion. Kesharwani and Agrawal found even greater changes. The second complication results from the existence, in CaF_2-type structures and with Γ_{5g} strains, of displacements of F ions which do not correspond to a uniform strain around the Ca site. These "additional" displacements have been pointed out for the first time and evaluated by Malkin and Ivanenko.[25] The mechanism of their creation is the following. The Γ_{5g} strains induce an electric field at the noncentrosymmetric site of F ions, which polarizes these ions and thus develops the displacements. If one considers only the $(CaF_8)^{6-}$ complex, these displacements correspond to one set of even normal modes associated with Γ_{5g}. The normal modes of this complex have been

studied by Huang and Inoue.[27] Nine of them are even, but only six, associated with Γ_{1g}, Γ_{3g}, $\Gamma_{5g}^{(1)}$ are usually considered the ones excitable by acoustic waves or uniform strains. The three others, associated with $\Gamma_{5g}^{(2)}$, are the "additional" displacements just discussed. They have been ignored until now for calculating relaxation rates and stress induced shifts because, in crystals having CsCl structure, they cannot be excited by a uniform strain. In CaF_2 structure, on the contrary, we have seen that they can. Of course, the values of these displacements are not the same for the F ions which are nearest neighbors of the rare-earth ion and for the others. Evaluations made by Malkin and Ivanenko for Yb^{3+} in CaF_2 show, for instance, that the former are 78% and the latter 50% of the "normal" stress-induced displacements.

We can try to take into account the existence of local elastic constants and these additional displacements by changing the values of the $B_i(\Gamma_\alpha, \beta)$ and of M of Eqs. (19) and (21), which we have deduced from the experiments using bulk elastic constants. As with Γ_{3g} strains the additional displacements do not exist, we have only to change the elastic constant $C_{11}-C_{12}$. We have seen, in Sec. IV E, that this quantity must be multiplied by 2 for the Newman model to be compatible with our results. Although no estimations have been made on $SrCl_2$ crystal, this factor seems very high as compared to the results on CaF_2. Regarding the case of Γ_{5g} strains, we have not tried to deduce the value of the additional displacements, as Baker and Van Ormondt did, for an agreement between our experiments and the Newman model because we have not an evaluation for the local elastic constants nor an estimation of the values of the t_i.

The electrostatic model discussed in Sec. IV F is strongly affected by the additional displacements. The theory developed in Ref. 5 can, however, be modified to take them into account. One can show that the number of independent quantities becomes five instead of three, the value of the displacement being one of them. With only five bits of experimental information, we have not a redundancy and thus we cannot test the validity of the model. In order to reduce to four the number of the unknowns, we plan to obtain the value of these displacements from the measurement of the electric field gradient seen by the Cl ions in the strained crystal. Here, we choose the following method: (i) we change the value of $B_7(\Gamma_{3g}, \theta)$ and $B_6(\Gamma_{3g}, \theta)$ by the same factor to take into account the existence of local elastic constants; (ii) we change the value of $B_7(\Gamma_{5g}, 0)$ and $B_6(\Gamma_{5g}, 0)$ by another factor to take into account the existence of local elastic constants and additional displacements; (iii) we change the value of M by a factor different from the previous one (although only Γ_{5g} strains are involved in the Γ_6 state's lifetime) to eventually correct the averaging of the sound velocity. These changes are made in order to get an agreement with the model, i.e., to describe the orbit lattice coupling with only three parameters (see Sec. IV F and Table II). The first factor, 1.25, is of correct order of magnitude. The second, 0.4, is plausible as it reflects both local elastic constants and additional displacements. The last, 0.8, is more surprising, since, being twice the previous one, it would mean that the value of the averaged sound velocity we have chosen must be reduced by a factor of[5] $\sqrt{2} = 1.15$. The values of these factors show that the model is not unreasonable. Nevertheless, its validity will not be tested before the problems of local elastic constants and of the additional displacements are solved.

H. Correlation between relaxation times and other measurements

As pointed out at the end of Sec. II, we have not tried to solve the complicated problem of finding the relaxation times associated with the direct process. From the calculations of Bernstein and Franceschetti[10] made for Ho^{2+} in CaF_2, we can see that a simplified treatment neglecting the hyperfine coupling would give bad results. The mixing introduced by that coupling is at least as important as that created by the Zeeman term. So, we cannot compare our results for the direct process with the stress results.

With the Orbach process, the situation is better. We ought again to build a system of 16 rate equations, but, as the hyperfine coupling is not responsible for this process, we can neglect it. We have seen in Sec. IV C that the calculation of the Γ_6 state's lifetime with the hyperfine coupling changes the factor 6 of Eq. (18), obtained by neglecting it, into 5.3. This change gives an order of magnitude of the error resulting from this neglect. With this approximation, it is easy to show that T_1 and T_2 for the ground Γ_7 doublet are given by

$$\frac{1}{T_1} = \tfrac{8}{3}\,\mathfrak{a}_5 M^2 f(\Delta_6) + 4f(\Delta_8)\,\frac{(K_3+K_4)(3K_5+K_4)+(K_3+K_5)(K_5+3K_4)}{2K_3+3K_5+3K_4} \tag{22}$$

and

$$1/T_2 = \tfrac{1}{2}\,\Delta\omega = 3\mathfrak{a}_5 M^2 f(\Delta_6) + f(\Delta_8)\,(2K_3+3K_4+3K_5)\,, \tag{23}$$

where

$$K_3 = \mathfrak{a}_3 \left| B_7(\Gamma_{3g}, \theta) \right|^2, \quad K_4 = \mathfrak{a}_4 \left| B_7(\Gamma_{4g}, 0) \right|^2,$$

$$K_5 = \mathfrak{a}_5 \left| B_7(\Gamma_{5g}, 0) \right|^2, \quad f(\Delta_i) = (\Delta_i/\hbar)^3 (e^{\Delta_i/kT} - 1)^{-1}.$$

$B_7(\Gamma_{3g}, \theta)$ and $B_7(\Gamma_{5g}, 0)$ have been defined in Sec. II. $B_7(\Gamma_{4g}, 0)$, which represents the effect of "ro-

tational modes," is given by

$$B_7(\Gamma_{4g},0)=\sum_l s_l \langle 7,\Gamma_8,-\tfrac{1}{2}|\, V(l,\Gamma_{4g}) \times O(l,\Gamma_{4g},0)|\,\Gamma_7,-\tfrac{1}{2}\rangle ,$$

and the α_i are the values of the quantity α of Eq. (20) obtained by the averaging method of Baker and Van Ormondt[4] (see Sec. IV C).

The values of $B_7(\Gamma_{3g},\theta)$, $B_7(\Gamma_{5g},0)$, and M, deduced from our uniaxial stress measurements and from the Γ_6 linewidth, are given by Eqs. (19a), (19b), and (21). The value of $B_7(\Gamma_{4g},0)$ cannot be obtained from any of our experiments. Its theoretical expression is

$$B_7(\Gamma_{4g},0)=[2.68V(4,\Gamma_{4g})-7.54V(6,\Gamma_{4g})]\times 10^{-2}$$

In the model developed in Ref. 5 we have shown that the parameters $V(l,\Gamma_{4g})$ are related to the static-crystal-field parameters by

$$V(4,\Gamma_{4g})=\sqrt{\tfrac{10}{3}}\,A(4,\Gamma_{1g}),\quad V(6,\Gamma_{4g})=\sqrt{7}\,A(6,\Gamma_{1g}).$$

Using the values given by Eq. (14) we obtain $B_7(\Gamma_{4g},0)=72\ \mathrm{cm}^{-1}$ and

$$1/T_1=1.37\times 10^9(e^{\Delta_6/kT}-1)^{-1}+10.6\times 10^9(e^{\Delta_8/kT}-1)^{-1}, \quad (24)$$

$$1/T_2=1.54\times 10^9(e^{\Delta_6/kT}-1)^{-1}+11\times 10^9(e^{\Delta_8/kT}-1)^{-1}. \quad (25)$$

The problem of the relation between T_1 and T_2 has recently been discussed by Stapleton and his colleagues.[17,18] For the Raman process, they found experimentally $T_1/T_2\sim 2$ for Kramers systems, and they used the relation $T_1=T_2$ for the correlation of their results in the case of an Orbach process. Equations (22) and (23) show that T_1 and T_2 are not equal and that they are even not proportional. We can mention that, if we ignore the contribution of the Γ_{4g} modes, the factors 10.6 and 11.0 become 5.3 and 7.4, giving a ratio $T_2/T_1=0.7$ for the part due to the Γ_8 quadruplet. Thus the near equality which appears in Eqs. (24) and (25) is only accidental. The comparison between the semitheoretical values (24) and (25) and the fitting of our experimental results by Eqs. (17) and (18) shows a good agreement for the part due to the Γ_6 doublet and a less good one for the part due to the Γ_8 quadruplet. The reason can lie in the fact that, in the former part, the averaging of the sound velocity has no influence since the calculated values (24) and (25) are obtained from the Γ_6 linewidth, while in the latter part we use uniaxial *static* stress results. Another reason can be the fact that the contribution of the rotational modes to the latter part has been calculated theoretically from the relations established in Ref. 5 within an electrostatic model. Finally, the difference by a factor of 2 between the T_1 and T_2 fitting laws for the Γ_8 contribution is in disagreement with the results (24) and (25) which show that the coefficients ought to be nearly equal. Attempts to fit our results for T_2 with the same law as for T_1 plus a Raman term were unsuccessful.

V. CONCLUSION

With the use of an effective spin Hamiltonian we have established analytical expressions giving, for any magnetic field and applied uniaxial stress orientations, the shift of EPR lines associated to a cubic doublet Γ_6 or Γ_7 when the hyperfine and Zeeman couplings are of the same order of magnitude. That was possible because a change in magnetic field direction does not modify the eigenvalues, but only the eigenstates of a cubic doublet. We have measured the uniaxial induced shift of EPR lines of Ho^{2+} in $SrCl_2$ for both the ground doublet and the first excited doublet. These results plus the lifetime of the excited doublet states give five bits of experimental information and thus make possible a test for some models which propose a parametrization of the orbit-lattice coupling. None of these are compatible with our results. The reason lies probably in the existence of local elastic constants near the paramagnetic ion and of particular atomic displacements typical of CaF_2-type structures. The measured relaxation times T_1 and T_2 of the ground doublet are compared with the values deduced from the static-stress experiments. The small disagreement can be attributed either to the method of averaging the sound velocity or to the evaluation of the rotational Γ_{4g} modes.

ACKNOWLEDGMENTS

We would like to thank Professor Chapelle of the Orsay University and Dr. Bill of the Genève University for giving us $SrCl_2$ crystals, J. C. Dumais for his help in relaxation-time measurements, and Dr. J. M. Baker for many helpful discussions and for bringing to our attention the works of B. Z. Malkin and his colleagues on the additional displacements in CaF_2 crystals. We would also thank Dr. Hennies for his collaboration during the first phase of this work and particularly for building the solid-electrolysis apparatus.

APPENDIX A

Normalized linear combinations used for the $\sigma(\Gamma_\alpha,\beta)$ are

$$\sigma(\Gamma_{3g},\theta)=(1/\sqrt{6})(2\sigma_{zz}-\sigma_{xx}-\sigma_{yy}),$$

$$\sigma(\Gamma_{3g},\epsilon)=(1/\sqrt{2})(\sigma_{xx}-\sigma_{yy}),$$

$$\sigma(\Gamma_{5g}\pm 1)=\mp(i/2)[\sigma_{yz}+\sigma_{zy}\pm i(\sigma_{xz}+\sigma_{zx})],$$

$$\sigma(\Gamma_{5g},0)=(i/\sqrt{2})(\sigma_{xy}+\sigma_{yx}),$$

$$\sigma(\Gamma_{5g}, yz) = (1/\sqrt{2})(\sigma_{yz} + \sigma_{zy}) ,$$

$$\sigma(\Gamma_{5g}, xz) = (1/\sqrt{2})(\sigma_{zx} + \sigma_{xz}) ,$$

$$\sigma(\Gamma_{5g}, xy) = \sigma(\Gamma_{5g}, 0)/i = 1/\sqrt{2}\ (\sigma_{xy} + \sigma_{yz}) .$$

There are two forms for the Γ_{5g} combinations. The first, which is complex, is the best when we calculate the matrix elements of the Hamiltonian (1); the second which is real, is the best when we transform the effective Hamiltonian (see Appendix B). The Γ_{4g} combinations, used only in Sec. IV H for calculating the Orbach relaxation time, can be deduced from the Γ_{5g} by substitution of $\sigma_{ij} - \sigma_{ji}$ for $\sigma_{ij} + \sigma_{ji}$.

APPENDIX B

The Hamiltonian $\mathcal{H}_{eff}$ contains terms in $H_i S_j$ and $I_i S_j$ whose transformation properties under the rotation $\mathcal{R}$ are

$$d^{-1}\mathcal{D}^{-1} H_i S_j \mathcal{D} d = H_i \sum_k R_{jk} S_k ,$$

$$d^{-1}\mathcal{D}^{-1} I_i S_j \mathcal{D}\, d = \sum_{k,l} R_{ik} R_{jl} I_k S_l ,$$

where R_{ij} are the matrix elements of the matrix R associated with the rotation $\mathcal{R}$. If we let $H_i = \mu_i H$, we can write $\tilde{\mathcal{H}}_{eff}$ of Eq. (8) as

$$\tilde{\mathcal{H}}_{eff} = \sum_{\alpha,\beta,i} g_J \mu_B H A_\alpha B_i^{\alpha\beta} S_i\, \sigma(\Gamma_\alpha, \beta) + \sum_{\substack{\alpha,\beta \\ i,j}} a A_\alpha T_{ij}^{\alpha\beta} I_i S_j \sigma(\Gamma_\alpha, \beta) ,$$

the row matrix $B^{\alpha\beta}$ being defined by

$$B_k^{\alpha\beta} = \sum_{ij} \mu_i \lambda_{ij}^{\alpha\beta} R_{jk} ,$$

and the square matrix $T^{\alpha\beta}$ by

$$T_{kl}^{\alpha\beta} = \sum_{ij} (R^{-1})_{ki} \lambda_{ij}^{\alpha\beta} R_{jl} .$$

Let (θ, ϕ) be the polar angles of $\vec{H}$ with respect to the cubic axis. Then

$$\mu = (\sin\theta\cos\phi \quad \sin\theta\sin\phi \quad \cos\theta) ,$$

$$R = \begin{pmatrix} \sin\phi & \cos\theta\cos\phi & \sin\theta\cos\phi \\ -\cos\phi & \cos\theta\sin\phi & \sin\theta\sin\phi \\ 0 & -\sin\theta & \cos\theta \end{pmatrix} ,$$

the B and T matrix being given by

$$B^{3,1} = (1/\sqrt{6})(0 \quad -\tfrac{3}{2}\sin 2\theta \quad 3\cos^2\theta - 1) ,$$

$$B^{3,2} = (1/\sqrt{2})(\sin\theta\sin 2\phi \quad \tfrac{1}{2}\sin 2\theta\cos 2\phi \quad \sin^2\theta\cos 2\phi) ,$$

$$B^{5,yz} = (1/\sqrt{2})(-\cos\theta\cos\phi \quad \cos 2\theta\sin\phi \quad \sin 2\theta\sin\phi) ,$$

$$B^{5,xz} = (1/\sqrt{2})(\cos\theta\sin\phi \quad \cos 2\theta\cos\phi \quad \sin 2\theta\cos\phi) ,$$

$$B^{5,xy} = (1/\sqrt{2})(-\sin\theta\cos 2\phi \quad \tfrac{1}{2}\sin 2\theta\sin 2\phi \quad \sin^2\theta\sin 2\phi) ,$$

$$B^{4,x} = (1/\sqrt{2})(-\cos\theta\cos\phi \quad \sin\phi \quad 0) ,$$

$$B^{4,y} = (1/\sqrt{2})(-\cos\theta\sin\phi \quad -\cos\phi \quad 0) ,$$

$$B^{4,z} = (1/\sqrt{2})(\sin\theta \quad 0 \quad 0) ,$$

$$T^{3,1} = \frac{1}{\sqrt{6}} \begin{pmatrix} -1 & 0 & 0 \\ 0 & 3\sin^2\theta - 1 & -3\sin\theta\cos\theta \\ 0 & -3\sin\theta\cos\theta & 3\cos^2\theta - 1 \end{pmatrix} , \quad T^{3,2} = \frac{1}{\sqrt{2}} \begin{pmatrix} -\cos 2\phi & \cos\theta\sin 2\phi & \sin\theta\sin 2\phi \\ \cos\theta\sin 2\phi & \cos^2\theta\cos 2\phi & \tfrac{1}{2}\sin 2\theta\cos 2\phi \\ \sin\theta\sin 2\phi & \tfrac{1}{2}\sin 2\theta\cos 2\phi & \sin^2\theta\cos 2\phi \end{pmatrix} ,$$

$$T^{5,yz} = \frac{1}{\sqrt{2}} \begin{pmatrix} 0 & \sin\theta\cos\phi & -\cos\theta\cos\phi \\ \sin\theta\cos\phi & -\sin 2\theta\sin\phi & \cos 2\theta\sin\phi \\ -\cos\theta\cos\phi & \cos 2\theta\sin\phi & \sin 2\theta\sin\phi \end{pmatrix} , \quad T^{5,xy} = \frac{1}{\sqrt{2}} \begin{pmatrix} -\sin 2\phi & -\cos\theta\cos 2\phi & -\sin\theta\cos 2\phi \\ -\cos\theta\cos 2\phi & \cos^2\theta\sin 2\phi & \tfrac{1}{2}\sin 2\theta\sin 2\phi \\ -\sin\theta\cos 2\phi & \tfrac{1}{2}\sin 2\theta\sin 2\phi & \sin^2\theta\sin 2\phi \end{pmatrix} ,$$

$$T^{5,xz} = \frac{1}{\sqrt{2}} \begin{pmatrix} 0 & -\sin\theta\sin\phi & \cos\theta\sin\phi \\ -\sin\theta\sin\phi & -\sin 2\theta\cos\phi & \cos 2\theta\cos\phi \\ \cos\theta\sin\phi & \cos 2\theta\cos\phi & \sin 2\theta\cos\phi \end{pmatrix} , \quad T^{4,x} = \frac{1}{\sqrt{2}} \begin{pmatrix} 0 & -\sin\theta\cos\phi & \cos\theta\cos\phi \\ \sin\theta\cos\phi & 0 & -\sin\phi \\ -\cos\theta\cos\phi & \sin\phi & 0 \end{pmatrix} ,$$

$$T^{4,y} = \frac{1}{\sqrt{2}} \begin{pmatrix} 0 & -\sin\theta\sin\phi & \cos\theta\sin\phi \\ \sin\theta\sin\phi & 0 & \cos\phi \\ -\cos\theta\sin\phi & -\cos\phi & 0 \end{pmatrix}, \quad T^{4,z} = \frac{1}{\sqrt{2}} \begin{pmatrix} 0 & -\cos\theta & -\sin\theta \\ \cos\theta & 0 & 0 \\ \sin\theta & 0 & 0 \end{pmatrix}.$$

*Laboratoire associé au Centre National de la Recherche Scientifique.

[1]D. J. Newman, Adv. Phys. 20, 197 (1971).
[2]Chao-Yuan Huang, Phys. Rev. 139, A241 (1965).
[3]M. Borg, R. Buisson, and C. Jacolin, Phys. Rev. B 1, 1917 (1970).
[4]J. M. Baker and D. Van Ormondt, J. Phys. C 7, 2060 (1974).
[5]R. Buisson, and M. Borg, Phys. Rev. B 1, 3577 (1970).
[6]J. M. Baker and G. Currel, Phys. Lett. A 28, 735 (1969), and *Colloques Internationaux du C.N.R.S.* No. 180, Vol. 2, (C.N.R.S., 1969).
[7]E. S. Sabisky, Phys. Rev. 141, 352 (1966), and Ph.D. thesis (University of Pennsylvania, 1965) (unpublished).
[8]H. A. Weakliem, and Z. J. Kiss, Phys. Rev. 157, 277 (1967).
[9]A. Abragam, J. F. Jacquinot, M. Chapellier, and M. Goldman, J. Phys. C 5, 2629 (1972).
[10]E. R. Bernstein, and D. R. Franceschetti, Phys. Rev. 9, 3678 (1974).
[11]H. Guggenheim, and J. V. Kane, Appl. Phys. Lett. 4, 172 (1964).
[12]F. K. Fong, J. Chem. Phys. 41, 1511 (1964).
[13]A. G. Danilov, J. C. Vial, and A. Manoogian, Phys. Rev. 8, 3124 (1973).
[14]F. R. Szofram, J. L. Smith, and G. Seidel, Phys. Lett. 42, 363 (1973).
[15]K. R. Lea, M. J. M. Leask, and W. P. Wolf, J. Phys. Chem. Solids 23, 1381 (1962).
[16]Le Si Dang, R. Buisson, and F. I. B. Williams, J. Phys. 35, 49 (1974).
[17]R. L. Marchand, and H. J. Stapleton, Phys. Rev. 9, 14 (1974).
[18]W. T. Gray, and H. J. Stapleton, Phys. Rev. B 9, 2863 (1974).
[19]H. V. Lauer, K. A. Solberg, D. H. Khonner, and W. E. Bron, Phys. Lett. A 35, 219 (1971).
[20]D. R. Huffman and M. H. Norwood, Phys. Rev. 117, 7091 (1960).
[21]Y. Luspin (private communication).
[22]J. C. Vial, thesis (University of Grenoble, 1973) (unpublished).
[23]Z. Sroubek, M. Tachiki, P. H. Zimmermann, and R. Orbach, Phys. Rev. 165, 435 (1968).
[24]C. H. Anderson, in *Crystals with the Fluorite Structure*, edited by W. Hayes (Oxford U.P., London, 1974).
[25]Z. I. Ivanenko, and B. Z. Malkin, Fiz. Tverd. Tela 11, 1859 (1969) [Sov. Phys.-Solid State 11, 1498 (1970)]; B. Z. Malkin, Z. I. Ivanenko, and I. B. Aizenberg, Fiz. Tverd. Tela 12, 1873 (1970) [Sov. Phys.-Solid State 12, 1491 (1971)]; B. Z. Malkin, Fiz. Tverd. Tela 11, 1208 (1969) [Sov. Phys.-Solid State 11, 981 (1970)].
[26]K. M. Kesharwani and B. K. Agrawal, Phys. Rev. B 9, 3630 (1974).
[27]C. Y. Huang and M. Inoue, J. Phys. Chem. Solids 25, 889 (1964).